TOWARDS THE DECONTAMINATION OF PLUTONIUM CONTAMINATED BRICKS: CREATION OF A CERIUM-BASED SIMULANT CONTAMINATION SYSTEM

James Kennedy[a,b], Colin Boxall[a], Anthony Banford[b], Rick Demmer[c], Andrew Parker[d]

[a]*Engineering Department, Lancaster University, Gillow Avenue, Lancaster, LA1 4YW, UK*
[b]*The Centre for Innovative Nuclear Decommissioning (CINDe), NNL, Havelock Road, Workington, CA14 3YQ, UK*
[c]*Idaho National Laboratory, PO Box 1625 MS 6150, Idaho Falls, ID 83415, USA*
[d]*The John Tyndall Nuclear Research Institute, University of Central Lancashire, Preston, Lancashire, PR1 2HE, UK*

Email: james.kennedy@nnl.co.uk, c.boxall@lancaster.ac.uk, anthony.w.banford@nnl.co.uk, rick.demmer@inl.gov, aparker11@uclan.ac.uk

There is a need for the decontamination of a number of plutonium-contaminated bricks encountered in a legacy BUTEX reprocessing plant on Sellafield site in the UK. Documentary review has indicated that the source of the contamination was a 8 mol dm^{-3} nitric acid process stream containing 10 mmol dm^{-3} of Pu in either the (III) or (IV) oxidation state.

Here we have sought to emulate the behaviour of Pu(III) by treatment of fired clay brick surfaces with a solution of 10 mmol dm^{-3} Ce(III) nitrate in 8 mol dm^{-3} nitric acid. XRD, porosimetry and EDX measurements of the untreated bricks reveal them to be comprised of low porosity silica and aluminosilicate phases with a surface layer of a low-Si content Al-C-N oxide derived from the atmosphere of the kiln in which the bricks were fired.

Depth profiling after an initial 6 week acid soak reveals that the acid penetrates <10 mm into the brick. SEM/EDX analysis reveals that acid treatment significantly roughens the brick surface due to dissolution the above described Al-C-N oxide layer. The EDX data also shows that virtually no Ce is retained as tenacious contamination at the brick surface; this may be due to a either a mass action/kinetic effect or taken to indicate that trivalent Ce(III) is less likely to absorb at the crystalline silica/aluminosilicate surface of the brick than its more easily hydrolysable tetravalent equivalent.

Preliminary higher-resolution EDX analysis indicates that small quantities of Ce(III) can be detected in pores or cracks on the surface of acid-treated brick samples. This suggests that Ce(III) may be non-tenaciously sequestered into surface defects – and that a simple salt wash may be sufficient to remove it. Based on the above observations, potential decontamination strategies are discussed and future studies outlined.

I. INTRODUCTION

Radiological decontamination is an essential enterprise that has become more important over the last four decades due to an increased focus on the decommissioning extant nuclear facilities as they reach the end of their design life. The costs and benefits of decontamination need to be balanced against the complete removal and demolition of contaminated areas or facilities. Demolition and removal are often the first options considered in such circumstances as decontamination may be thought of as slow and costly. Decontamination has advantages, including significant waste reduction over demolition.[1]

Different contamination scenarios have led to the development of hundreds of decontamination processes. Their selection balances criteria such as cost-effectiveness and waste minimization. Whilst testing on the actual systems where the contamination arises (as "field" radioactive specimens) is appropriate, doing so is often expensive, time-consuming and fraught with risk related to operator exposure. Simulating contamination with non-active contaminant simulants and substitute substrates provides a less expensive, radiologically safer, more controlled and often more informative means of decontamination method selection. Properly implemented, simulant-based studies both require and provide a unique understanding of the system.

In a previous study[2], we have developed a physico-chemical understanding of the factors affecting the decontamination efficiency for the removal of tenacious (americium, cobalt) and non-tenacious (caesium, strontium) contaminants from commonly used mineral-based industrial building materials. These include concrete and granite (in service to the decontamination and clean-up of redundant nuclear facilities) and predominantly urban building materials such as limestone and marble (in service to large scale remediation after a terrorist attack).

This work involved the development of representative non-active simulants for Cs, Sr, Am and Co as common radioactive contaminants and an extensive trialling of decontamination techniques on these simulants

in order to identify the most efficient contamination removal method. Simulant results were then validated in real radioactive decontamination scenarios.

With respect to the contaminants themselves, it was found that cations that exhibit pH-dependent speciation, such as americium or cobalt, can demonstrate radionuclide / material substrate specific chemistry that results in contaminant precipitation at the substrate surface, especially if the material has an intrinsically alkaline surface pH. For example, in the case of Am and Co, this results in the precipitation of Am and Co oxyhydroxide species at the outer surface of materials such as concrete with consequently high percentage removal efficiencies during attritive decontamination.

For cationic radionuclides such as Cs^+ that do not exhibit any nuclide/material surface specific chemistry, it was found that the principal material property controlling the tenacity of that nuclide during decontamination from the four substrates studied is the permeability of that substrate – with limestone, as the most permeable material studied, typically exhibiting the lowest decontamination efficiency for Cs^+.

For substrates of similar permeability such as granite, concrete and marble, it was found that net surface negative charge on the material substrate plays a major role in determining the tenacity of non-reactive cations such as Cs^+; the larger the net negative charge on the substrate surface, the more tenacious the contamination.

Finally, with respect to the decontamination agents themselves, harsh, high concentration chemical agents that utilize multiple decontamination processes (acids, bases, chelants) typically have an effectiveness advantage over more dilute, one component solutions. Strongly acidic solutions achieve the highest overall % removal decontamination results. This is partly because they tend to dissolve small amounts of the substrate surface and liberate imbibed contaminants. Finally, some strippable coating based methods are found to be surprisingly effective; likely because of their chelant / absorptive character.

Here, we seek to extend this work to plutonium as contaminant and fired clay brick as substrate. Specifically, we seek to identify and / or design an effective method for the decontamination of radioactively contaminated bricks and especially a number of plutonium-contaminated bricks encountered in a legacy BUTEX reprocessing plant on the Sellafield nuclear-licensed site in the UK.

As such, this work has two objectives: (i) the design and development of a representative simulant; and (ii) informed by the design criteria of the simulant, the selection of candidate decontamination techniques and their trialling in deployment. This, in turn, requires an understanding of the chemistry of the source of the contamination, key materials properties of the substrate contaminated, and the means by which they interacted during the contamination event.

The work described in this paper relates to the first of these objectives i.e. the design and production of a representative simulant. Specifically, we are seeking to simulate the effects of a plutonium nitrate / nitric acid solution on the structure of predominantly aluminosilicate fired clay-based engineering bricks representative of those used on Sellafield Site. As such, we propose to use cerium nitrate in nitric acid solution as a non-active surrogate for the Pu-loaded contaminating solution. The rationale behind this, in the context of contaminant chemistry, substrate properties and their interaction is as follows.

I.A. Nature of the Contamination

As stated above, the contaminated bricks that are the subject of this work are located in a building that forms part of a legacy BUTEX First Generation Reprocessing plant on Sellafield Site. This plant was constructed in the early 1950s to process and purify plutonium generated from the Windscale Piles.[3-8] The chemistry and operation of the process can be summarized as follows.

First developed at Chalk River the BUTEX process involves the dissolution of fuel elements in nitric acid, a primary U/Pu separation using 1-[2-(2-butoxyethoxy) ethoxy] as a solvent, followed by U and Pu product purification and finishing stages using TBP/OK as a solvent.[9-13] A simplified flow diagram for the BUTEX process is shown in Figure 1.

Implementation at Sellafield was as follows. After a period in delay storage to allow for cooling, fuel elements taken from the Windscale Piles were dissolved in concentrated nitric acid. The resultant highly active feed stream was then passed to the primary separations process where the fission products were removed and the majority of the uranium separated from the plutonium. The fission products would then go through a separate cycle of processing before final vitrification. The uranium and plutonium streams would continue onto separate purification cycles for processing.[8,9]

The plutonium purification process (highlighted with a red dashed line in Figure 1) was split into two steps. As implemented at Sellafield, the fuel dissolution, primary separation process & first step of the plutonium purification process and the second step of the plutonium purification process took place in two separate but adjoining buildings referred to as the Primary Separation Plant (PSP) and Plutonium Purification Plant (PPP) respectively. The contaminated bricks to be studied here are located in the PPP.

Due to being located in adjoining buildings, the two steps of the plutonium purification process were physically separate from one another. The initial step of the purification cycle took place within the PSP, during which the BUTEX solvent was removed from the plutonium

stream.[8,9] This 1st cycle consisted of an oxidation, two extraction columns and an evaporator to concentrate the Pu-bearing liquor prior to it being passed to the 2nd cycle. The removal of the BUTEX solvent prior to the Pu stream being passed to the PPP allows for solvent participation to be discounted from the contamination event that occurred within the PPP. As well, the fact that this process stream was comprised only of Pu in nitric further simplifies the chemistry to be considered in understanding the contamination event itself.

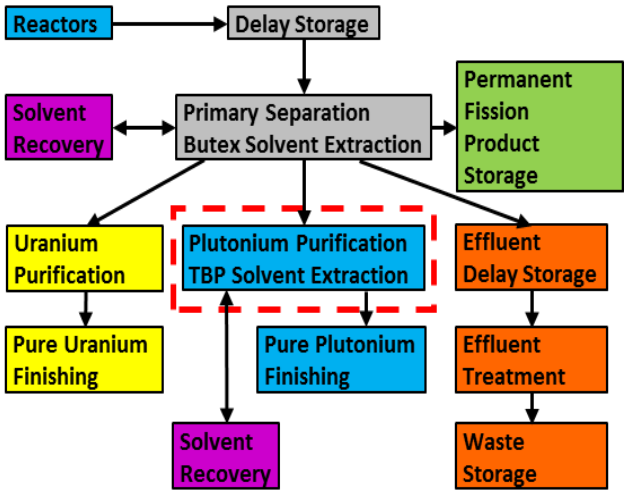

Figure 1: Simplified flow sheet of the BUTEX process. Sourced from *Gray et al*[9]

This aqueous plutonium-in-nitric acid stream then continued on to the second cycle of the purification process which, as described above, took place in the adjoining PPP. In this cycle, the plutonium-bearing liquor from the first cycle entered a batch conditioner where the liquor acidity was adjusted. From here the plutonium stream yet again passed through two extraction columns and any remaining contaminants were removed. The plutonium-bearing liquor was then concentrated, prior to transfer to the Plutonium Finishing Plant (PFP) where the plutonium metal was finally extracted.[8,9]

Like much of the BUTEX plant the PPP building, designed solely to purify plutonium nitrate solutions from the PSP, was commissioned in 1952. Its operation was superseded in 1964 when other facilities came online at Sellafield. However, it continued to be used to recover plutonium from residues such as mixed oxides, flourides and nitrates from elsewhere on site although the chemistry of the process remained unchanged. It was eventually closed in 1987.

Since then, much of the process plant has been stripped out, leaving only a brickwork shell, part of which has been contaminated by plutonium. It is not unreasonable to assume that this contamination arose due to a leak / escape of process liquor at some point during the operational period of the building. However, the removal of the process pipework and vessels makes it difficult to correlate the location of the contamination to vessels or pipework containing a specific process stream

This difficulty notwithstanding, a review of the schematics of the two stages involved in the purification process after primary separation did allow for the composition of the likely contaminant to be determined – specifically a solution of 10 mmol dm^{-3} Pu in 8 mol dm^{-3} nitric acid, with the Pu most likely in a mixture of the (III) and (IV) state. This information then allowed for the design the first of our non-active simulants for the contamination source. In order to deconvolute effects due to Pu(III) and Pu(IV), we first focused on the former by use of a simulant comprised of Ce(III) nitrate in 8 mol dm^{-3} nitric acid. Beyond the scope of this communication, the effect of Pu(IV) will be interrogated subsequently through use of Ce(IV) as a simulant.

I.B. Composition of Fire Clay Bricks

Having identified both the source of the contaminant (a process stream of 10 mmol dm^{-3} Pu in 8 mol dm^{-3}) and the most likely means of contamination (escape or leak of the process stream onto the brick surface), our attention turned to the brick substrate itself – particularly with regards to understanding the effects of the acid leaching on brick chemistry and structure.

The raw ingredients for bricks are clay or shale, small aggregate such as sand, and fluxing agents such as lime and ferric oxide – the latter resulting in a more reliable firing process.[14]

The clay for the bricks is predominantly an alumina-silicate, with varying other elements depending on clay composition. The type and composition of clay used in the manufacture of bricks depends greatly on the intended use of the brick as well as the region in which the clay has been sourced. While clays are very abundant, only a few are suitable for brick manufacturing.[15,16]

Fired clay-based brick normally contains between 50 and 60% silica (predominantly from the sand), 20-30% alumina (from the clay) and approximately 7% iron oxides and other trace elements, mainly from the fluxes used in the manufacturing – along with haematite that is formed during the firing process.[14,15,17,18]

The engineering bricks used as substrate simulants in the experimental part of this study are a porous vitrified ceramic[14], more akin to a glass or glass-ceramic than a cement due to their high firing temperature of up to 1400ºC. During their firing, or more accurately vitrification, the liquid glass fills some of the pores within the brick and therefore reduces the porosity of the brick structure.[14] The extent of vitrification is dependent on the temperature and length of the firing process. The amount of vitrification can be increased by adding fluxing agents to the mix such as feldspar (also an aluminosilicate).[14,15]

Increasing the amount of vitrification within the brick results in a more durable brick with lower porosity.[14]

The engineering bricks used in this study have a high glass content; thus concepts applied to the understanding of glass corrosion will also be of relevance here – especially when simulating the contamination of the brick by exposing it to a solution of cerium nitrate in 8 mol dm^{-3} nitric acid. In summary, corrosion of glass in water is caused by ion exchange between H^+ species in the water and alkali ions in the glass.[19] Glass is known to dissolve slowly but irreversibly in water forming a hydrated glass gel (silica hydroxide) species and an aqueous (H_2SiO_3) species.[20] As the brick structure in this study will be exposed to concentrated nitric acid, this mechanism is likely to cause significant damage to the vitrified sections of the brick.

Having reviewed the key features of the contaminated substrate, as well as having determined the composition of the contaminating process stream itself, we can now move to create a simulant system. This is the subject of the remainder of this paper.

II. EXPERIMENTAL

II.A Materials

All chemicals used were of AnalaR grade or better and supplied by Sigma Aldrich (Gillingham, Dorset, UK), with exception of the cerium nitrate supplied by American Elements (Los Angeles, USA). All H_2O used was ultrapure from a Direct-Q 3 UV Millipore water purification system (Millipore, Watford, UK) to a resistivity of 18.2 MΩ.cm.

The contaminated BUTEX facility described above was constructed using engineering bricks produced by the Whitehaven Brick & Tile Co. This ceased trading in the 1960s and thus any extant accessible samples of so-called Whitehaven Bricks from around Sellafield Site have undergone varying amounts of extensive and ill-documented weathering. Thus, in order to provide a consistent and well-characterized test system with a similarly complex composition as historical Whitehaven Bricks, the decision was taken to use modern Class B engineering bricks as the primary test substrate in these studies (manufactured by Wienerberger AG and supplied by Travis Perkins PLC. Product number 462691).

II.B Brick Analysis

Both before and after leaching tests (see section II.C below), brick samples were analysed using Scanning Electron Microscopy-Energy Dispersive X-Ray Analysis (SEM-EDX), Mercury Intrusion Porosimetry and Powder X-Ray Diffraction (XRD) Analysis as follows.

II.B.I SEM-EDX Analysis

SEM imaging of the bricks was carried out at 20 keV using the secondary electron imaging detector (SEI) of a JSM-6010PLUS scanning electron microscope (JEOL, Japan). EDX analysis of the bricks was carried out at 20 keV in the same microscope using a JEOL proprietary silicon drift detector (SDD), energy dispersive X-ray analyser.

II.B.II Mercury Intrusion Porosimetry

Using a bench top tile saw, brick samples were dry cut into "fingers" approximately 8mm in diameter and 20mm in length for pre-leaching analysis of porosity and permeability by Mercury Intrusion Porosimetry. This was conducted at the Centre for Infrastructure Management, Sheffield Hallam University, using a PASCAL 140/240 Mercury Intrusion Porosimeter (Thermo Fisher Scientific, USA). Tests were run with a maximum test pressure of 200 MPa, an increase speed of 9-14 MPa/min, and a decrease speed of 9-28 MPa/min.

II.B.III Powder XRD

Additionally, a sample of brick was crushed with a hammer and pulverised for subsequent analysis of mineralogical composition using powder XRD. A Bruker D2 PHASER X-ray diffractometer (Bruker, USA) mounted in a parallel beam configuration and using a Cu X-ray target (30 kV, 10 mA) with a kα wavelength of 1.54059 Å and kβ wavelength of 1.54184 Å was used. Scans were collected from 5° to 120° 2Theta at step intervals of 0.05°. Samples were run un-monochromated to improve the signal-to-noise ratio.

II.C Leaching Tests

As discussed at the end of section I.A, a candidate simulant for the source of the contamination for the Pu-contaminated bricks under study here is a solution of 10 mmol dm^{-3} cerium (III) nitrate in 8 mol dm^{-3} nitric acid. Accordingly, an experiment was designed to determine the effects of this simulant on the surface and interior structure of a representative brick. The experiment involved exposure of the bricks to both cerium loaded and cerium-free solutions in order to assess the effect of the acid alone on brick integrity.

II.C.I Sample Preparation

Ten of the engineering bricks described above, were each cut into eight 50 mm cubes using a wet cut diamond blade masonry saw. This provided the necessary number of samples plus some spare.

The bricks each have a smooth "glazed" and rough "non-glazed" surface, each of which needed to be tested. The "glazed" surface of the brick is simply formed

by applying a sand-free slurry of water and clay to the brick surface prior to firing.[21] It is, therefore, not strictly speaking a glaze. As the clay for the slurry is the same clay as used in the bulk of the brick, it is almost identical in elemental terms to the "non-glazed" surface.

In order to ensure that only the test surfaces were exposed to the acid, the "non-test" sides of the brick samples were coated in chemical resistant paint (Rawlins 310 Chemical Resistant Coating), see Figs 2 & 3.

II.C.II Test Solution Preparation

The test solutions used in the soaking experiments were made up as follows:
8 mol dm^{-3} nitric acid: 509.64 cm^3 of 70% nitric acid was added slowly to 250 cm^3 of deionized water in a 1 dm^3 volumetric flask. The flask was then filled to level with deionized water. The solution was then transferred to a storage flask.
10 mmol dm^{-3} Ce(III) nitrate in 8 mol dm^{-3} nitric acid solution: 509.64 cm^3 of 70% nitric acid was added slowly to 250 cm^3 of deionized water in a 1 dm^3 volumetric flask. To this 4.35g of cerium(III) hexahydrate was added. The flask was then filled to level with deionized water. The solution was then transferred to a storage flask.

II.C.III Soaking Procedure

The brick samples were placed in Pyrex soaking vessels (1.6L casserole dish, Wilko, UK) and were sat on "feet" made from small squares of ceramic tile. This is in order to lift the bottom of the sample off of the soaking vessel and allow the acid to contact the test surface. Both glazed and unglazed surfaces were separately presented to the soaking solution. Approximately 300ml of the test solution is added to the soaking vessel.

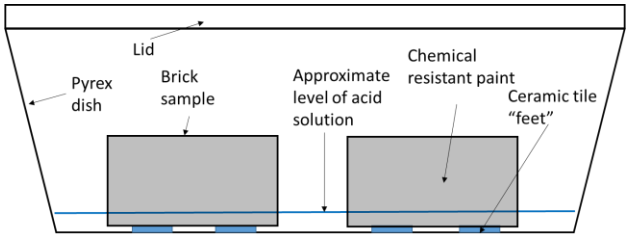

Figure 2: Diagram of the experimental setup showing the placement of samples in the test solution. (Note: the vessel held 4 brick samples, size enlarged for clarity)

A 10% solution change was carried out periodically to prevent saturation of the test solution by leached material. A lid and gasket made from XTS 320 Chemical Resistant Sealant (Intek Adhesives, UK) were used to limit the evaporation of the solution. The samples are left in the solutions for varying periods of time. These were 1 day, and 1, 3 and 6 weeks. Figure 2 shows a sketch of the soaking vessel setup.

II.C.IV Post Soaking Analysis Preparation

Once the brick samples had been soaked for the allotted period of time, they were taken out of the acid solution and allowed to air dry for a period of several weeks. The bricks received an additional oven drying of approximately 50°C for a period 5-6 hours, in order to ensure that all the acid had evaporated prior to analysis. When the brick samples were dry they were then cut in half using a diamond edge masonry chop saw. The samples were dry cut in order to prevent cutting fluid washing away any surface deposits. Brick samples were cut along the yellow line shown in Figure 3.

Figure 3: Image of brick sample cube coated in chemical resistant paint. Cutline highlighted, test face on top.

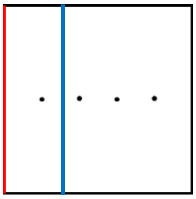

Figure 4: Diagram of a dissected cube with a red line indicating soaking face. Dots representing the 10 – 40mm marks.

II.C.V Analysis of Samples

Analysis was carried out on the interior of the sample using SEM/EDX at spots at distances of 10, 20, 30 and 40mm depth into the brick from the test surface as shown in Figure 4. This was done in order to determine the penetration depth of the nitric/Ce(III) solutions. Analysis of the test surface of the brick samples (glazed and unglazed) was also carried out. To do this, one of the dissected halves was again dissected using a chisel along the blue line shown in Figure 4 so that the sample could be accommodated in the SEM chamber. The test surface of the sample was then analysed using SEM and EDX.

III. RESULTS AND DISCUSSION

III.A Analysis of Un-Soaked Brick Samples.

Analysis of the non-soaked brick samples was performed using Mercury Intrusion Porosimetry. Results from five randomly selected samples (with associated sample serial numbers) are shown in Figure 5 from which it can be seen that the batch of engineering bricks purchased for this study has a consistent porosity of ~11% with a range of 10.07% to 11.88%. In addition, the pore size measured from these samples is also consistent with

the majority of pore size diameters falling in the range 0.2 to 1.5 μm.

The results of the powder XRD analysis of un-soaked samples, along with EDX-based elemental analysis of the samples (see later) are useful in determining the baseline composition of the brick. The XRD spectra and resultant chart of percentage composition of a representative brick sample are shown below in Figure 6. Colour coded species identification and percentage assignment were achieved using the XRD instrument's on-board data analysis software.

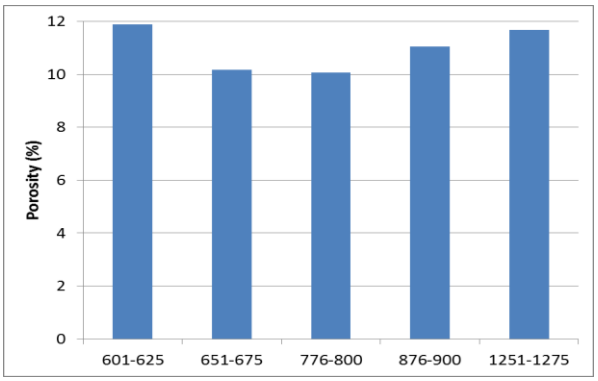

Figure 5. Graph of percentage porosity for 5 randomly selected brick samples. The values given on the x-axis simply corresponds to the sample serial number.

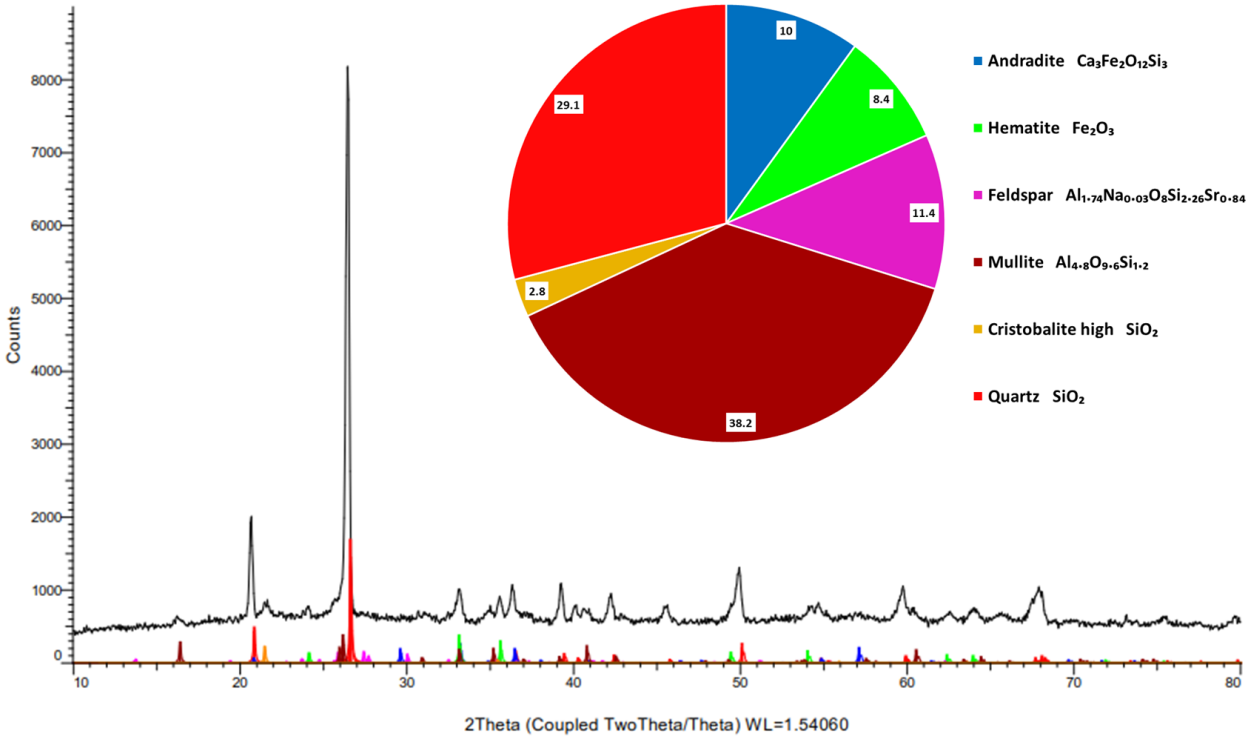

Figure 6. XRD spectra of a representative brick sample, pre-soaking with inset pie chart showing percentage composition of the sample. Includes colour coded species identification.

As expected, and based on the strong reflections at 21, 27, 60 and 70°, the two largest constituent phases are an aluminosilicate (consistent with mullite) and a crystalline silicon dioxide species (consistent with quartz), predominantly derived from the clay and sand respectively. These results compare well with the literature in regard to the silica and alumina compositions of brick being ~50% silica species and ~30% alumina species.[14,15,17,18] Other minority species such as feldspar and haematite are also present as a result of the flux used to improve the firing efficiency.

III.B Analysis of Soaked Brick Samples

III.B.I Effects on Interior of the Sample

In the first instance, the effect of the acid soak on the interior of brick samples was assessed. From the depth penetration analysis carried out by EDX on the bricks, it is clear the acid solutions have not penetrated to any significant depth. The graph in Figure 7 below shows the EDX-determined elemental composition at the 10 mm depth point for the 1 day and 6-week leaching times.

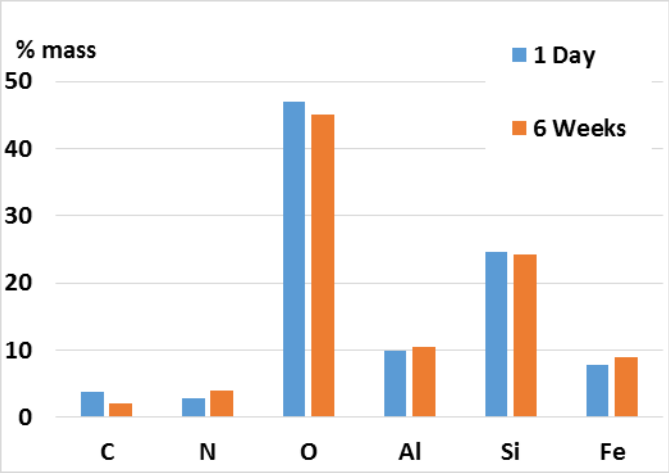

Figure 7: Chart of the main elements for the 1 day and 6-week acid soaked brick at 1mm depth.

From this it can be seen that there is very little change in the elemental composition of the sample over the 6 week soak period, suggesting that the acid has penetrated <10mm into the brick. Therefore the primary focus in regard to the effects the acid solutions have had on the bricks should be on the test surface of the samples.

This observation is useful for the design or selection of decontamination methods for this system as it shows that the contaminant is likely restricted to the surface of the bricks or the first few millimetres below the surface. As a result, this significantly reduces the amount of material needed to be physically attrited from the bricks if a chemical decontamination system proves to be less useful.

III.B.I Effects on the Exterior of the Samples.

Thus, the effects of the 8 mol dm^{-3} acid and 10 mmol dm^{-3} / 8 mol dm^{-3} acid soaks on the glazed and unglazed surfaces of the bricks was assessed.

The seven classes of samples soaked/unsoaked and analysed by SEM/EDX, as well as the letter code associated with each sample class, are as follows:

1. GNS – "glazed" surface, non-soaked,
2. NGNS – "non-glazed" surface non-soaked,
3. GAS – "glazed" surface soaked in acid only;
4. NGAS – "non-glazed" soaked in acid only;
5. GCS – "glazed" surface soaked in Ce(III) / acid solution;
6. NGCS – "non-glazed" surface soaked in Ce(III) / acid solution.
7. BNS – bulk material un-soaked (as a reference);

Those four sample classes that were soaked in acid or Ce(III)/acid solutions were each immersed for a period of 6 weeks in an attempt to maximise any observable changes in the physical condition or elemental composition.

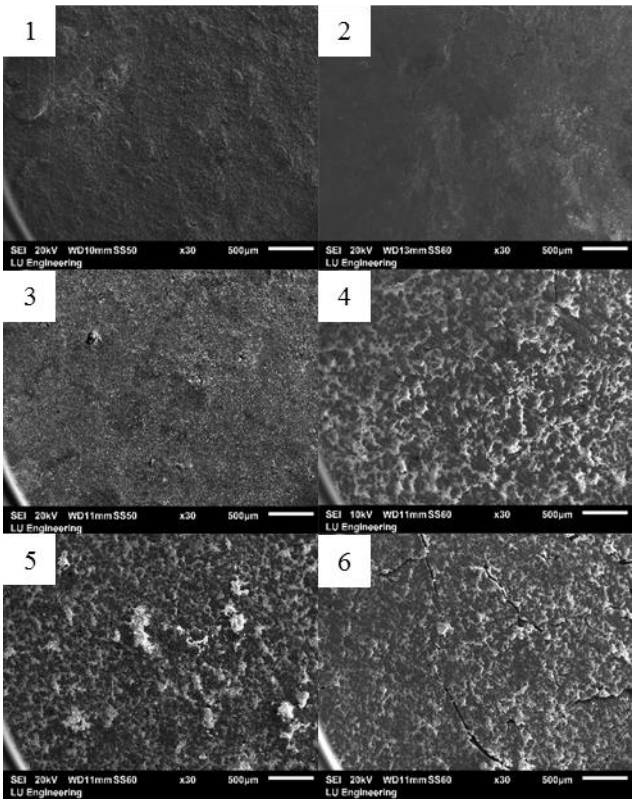

Figure 8: SEM images of the following samples: 1. NGNS; 2. GNS; 3. NGAS; 4. GAS; 5. NGCS; 6. GCS

Figure 8 shows SEM images taken from samples from classes 1-6 i.e. "glazed" and non-glazed surfaces, unsoaked, acid soaked and Ce(III)/acid soaked respectively. From this, it can be seen that all acid and Ce(III)/acid soaked samples exhibit significantly greater surface roughness than the unsoaked samples – due either to surface dissolution or reprecipitation processes or both. This roughness seems to be localised to the surface of the brick samples, as might be expected on the earlier observation that the acid penetrates only a few millimetres into the brick.

Figure 9 shows the results of the EDX elemental analysis, expressed as an average percentage mass, of the samples shown in Figure 10 as well as the composition of a BNS sample taken from the bulk/interior of an unsoaked brick as baseline.

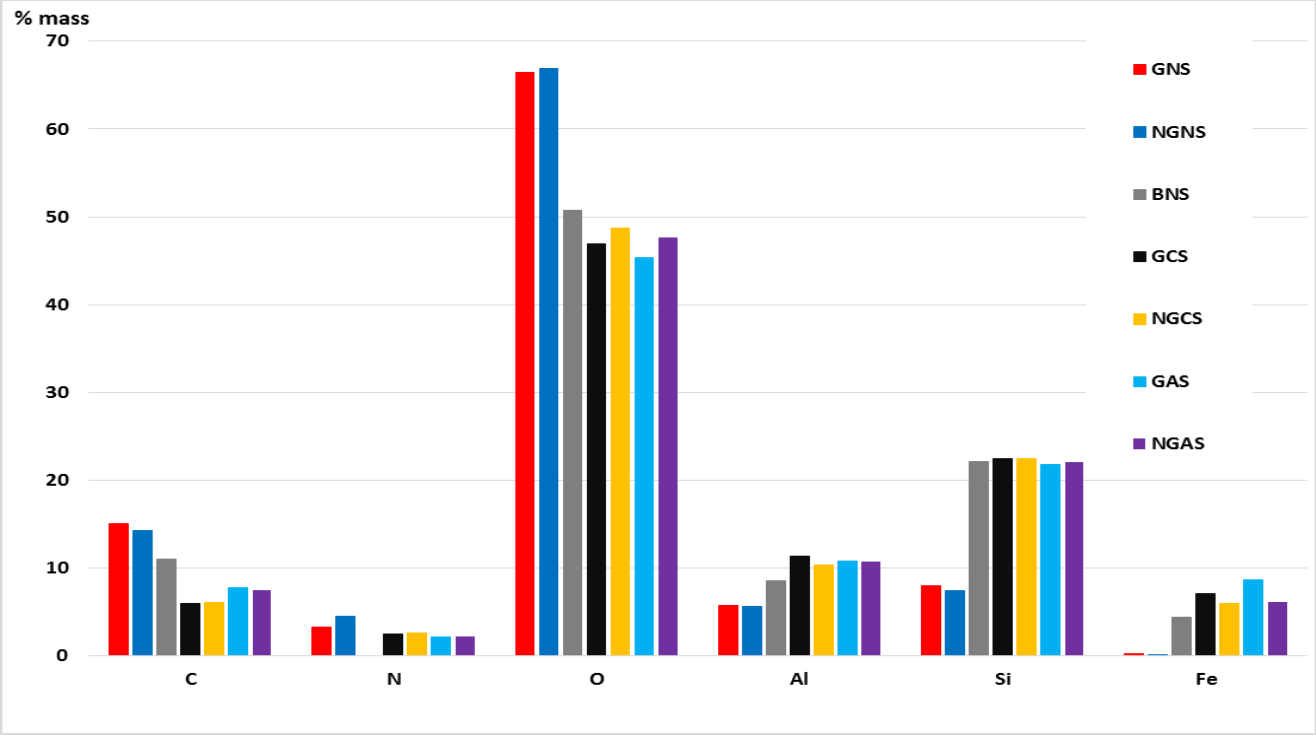

Figure 9: Elemental comparison of major elements of brick samples before and after soaking in test solutions for 6 weeks.

The carbon content of brick surfaces from the non-soaked sample classes, GNS and NGNS, are very similar, with the carbon originating predominantly from CO_2 from the gas-fired kiln used to fire the bricks but also from organic material in the clay as well as. The carbon content of the BNS class samples is lower than that of the GNS and NGNS samples due to it being isolated from the CO_2 in the kiln. The reduction in carbon content in the soaked samples is as a result of the atmospheric CO_2-derived carbon-containing minerals being dissolved and scoured off of the brick by the acid. Interestingly, the Ce(III) containing solution is more effective in removing the surface carbon than the acid only solution, although the reason for this is currently unclear.

Both the GNS and NGNS samples exhibit the presence of the nitrogen and this can be again explained as being a result of the absorption of NO_x compounds within the kiln. No nitrogen is observed in the BNS sample, again because of the isolation of the interior of the bricks from the kiln atmosphere. This result again speaks to the low permeability of the bricks suggested by the results of Figure 5. The nitrogen content detected from the GAS, NGAS, GCS and NGCS samples can then be attributed to the action of nitric acid on the brick surface.

The high oxygen content at the surface of the un-soaked GNS and NGNS samples is likely to have a significant contribution from the CO_2 and NO_x derived compounds produced during the firing process. That all four acid and Ce(III)/acid soaked samples exhibit lower oxygen contents than the GNS and NGNS samples, and that these soaked sample oxygen contents are similar to that of the BNS sample suggests that the soaking process is removing these compounds, revealing an underlying surface whose composition more closely reflects that of the brick interior.

The silicon concentration at the surface of the GNS and NGNS surface samples is low compared to the brick interior. This is expected in the case of the GNS sample due to the lack of sand and hence SiO_2 in the surface glaze of the brick (as mentioned above the "glaze" is a clay slurry). However, the low Si content for the NGNS sample is surprising and perhaps reflects the low silicon content in the kiln CO_2/NO_X derived surface layer on these non-soaked samples. Similar to the decrease in surface oxygen content observed upon soaking, the increase in relative Si content after leaching demonstrates that the surface of the brick samples has been significantly damaged to the point where the underlying matrix is exposed. This is clearly indicated by the almost identical Si content shown by the non- soaked bulk and the post soaked samples.

The soaking-induced changes in the aluminium and iron content at the surfaces of the samples studied in Figure 9, and the correlation of the concentrations of these elements at the surfaces of the soaked samples with those observed from the brick interior has much in common with the changes in silicon content described above. Specifically, Fe and Al lean layers have been removed

from the surface of the brick by acid treatment, resulting in the exposure of the underlying brick matrix.

However, the Al and particularly the Fe content of the post soaked samples is noticeably different from the un-soaked bulk sample and therefore, suggests that there is more occurring than surface layer removal alone. As noted in Jantzen et al[20] and Poluektov et al[22] amorphous and crystalline precipitates form during the corrosion process of glass and ceramic materials. These precipitates take the form of amorphous $Fe(OH)_3$ and cystalline Al and Fe containing saponite species[20] as well as others such as $CaAl_2Si_2O_8$ and $Al_2(Si_2O_5)(OH)_4$. If these bricks are indeed corroding in a manner analogous to that of glass as postulated above, this may explain the relative increase in Al and Fe content at the surface and suggests that Fe species are more likely to re-precipitate based on the larger relative increase in Fe content on acid treatment.

No cerium was detected on the surface of the brick samples after soaking. Whilst the Ce(III) concentration in the simulant solutions is representative of the concentration of Pu in the contaminating solution, it may be that a mass action effect is in operation i.e. the Ce(III) concentration is simply too low to absorbed at the brick surface in sufficient quantities to detected by EDX over the time scale of the experiments described here. Alternatively, it may be that the trivalent cation (Ce(III) or Pu(III)) is less likely to absorb at the corroded brick surface than its more easily hydrolysable tetravalent equivalent (Ce(IV) or Pu(IV)).

The results from Figures 10 and 11 both indicate the formation of surface precipitates upon acid treatment, presenting a potential issue in regard to future decontamination studies. It is possible that the Ce may either be incorporated within a layer of surface precipitates or under a layer of surface precipitates depending on the rate of formation.

Supporting the latter postulate, a preliminary re-analysis of the Ce(III)-soaked samples at higher spatial resolution (not shown) has indicated that ~0.5 wt% Ce could be detected in cracks at the surface of the "glazed" samples. Too, ~0.12 wt% Ce was detected in pores at the surface of the non-glazed" samples. This suggests that the cerium (and thus Pu) may sit non-tenaciously within the cracks and pores of the bricks rather than being chemically and tenaciously adhered to the brick surface. If this is indeed the case, it will may substantially simplify the decontamination process.

In order to test this, a second round of testing is being conducted. This testing will use a cerium concentration of 1 mol dm^{-3}, in order to allow for ease-of-detection. This will allow for speciation of the cerium to be carried out using Raman and XPS techniques. Once the cerium speciation has been established then work can commence on the development and testing of decontamination methods/ solutions.

IV. CONCLUSIONS

We have attempted to simulate Pu contaminated bricks found in a legacy BUTEX First Generation Reprocessing Plant on Sellafield site. Documentary review has indicated that the source of the contamination was a 8 mol dm^{-3} nitric acid process stream containing 10 mmol dm^{-3} of Pu in either the (III) or (IV) oxidation state.

In the first instance, we have sought to emulate the behaviour of Pu(III) by treatment of fired clay brick surfaces with a solution of 10 mmol dm^{-3} Ce(III) nitrate in 8 mol dm^{-3} nitric acid. XRD, mercury porosimetry and EDX measurements of the untreated bricks reveal them to be primarily comprised of low porosity crystalline silica and aluminosilicate phases with a surface layer of a low-Si content Al-C-N oxide, the carbon and nitrogen being primarily derived from the atmosphere of the kiln in which the bricks were fired.

EDX-based depth profiling of the bricks after an initial 6 week acid soak reveals that the acid penetrates <10 mm into the brick interior – as might be expected from the composition and porosity data. This is useful information in regard to design of a decontamination strategy, as it does not require a chemically based method to permeate a significant depth into the brick. In addition, if a chemical based decontamination solution is not ultimately practical, then only a thin layer of surface material would need to be removed by mechanical means.

SEM/EDX analysis reveals that acid treatment roughens the brick surface due to dissolution the above described Al-C-N oxide layer. EDX data also shows that virtually no Ce is retained as tenacious contamination at the brick surface; this may be due to a either a mass action/kinetic effect or taken to indicate that trivalent Ce(III) is less likely to absorb at the crystalline silica/aluminosilicate surface of the brick than its more easily hydrolysable tetravalent equivalent. These issues will be addressed in the next round of testing by (i) working at higher concentrations of Ce(III) in the contaminating solution and (ii) exploring the behaviour of Ce(IV).

Preliminary higher-resolution EDX analysis indicates that small quantities of Ce(III) can be detected in pores or cracks on the surface of acid-treated brick samples. This suggests that, whilst not chemically adhered to the brick surface, Ce(III) may be non-tenaciously sequestered into surface defects – and that a simple salt wash may be sufficient to remove it. This also will be the subject of further study.

ACKNOWLEDGEMENTS

The authors thank the UK Engineering & Physical Sciences Research Council (EPSRC) and the UK National Nuclear Laboratory (Award No. 17100013 and Agreement No NNL/UA/1017 respectively) for the provision of an iCASE PhD studentship for JK. This work

has been supported by the Centre for Innovative Nuclear Decommissioning (CINDe), which is led by the National Nuclear Laboratory, in partnership with Sellafield Ltd and a network of Universities that includes Lancaster University, the University of Manchester, the University of Liverpool and the University of Cumbria. Part of the work was conducted in Lancaster University's UTGARD Lab (Uranium / Thorium beta-Gamma Active R&D Lab), a National Nuclear User Facility supported by the EPSRC. The authors also thank the Lloyd's Register Foundation (award no. G0025) for support for CB. The Lloyds Register Foundation is an independent charity that supports the advancement of engineering-related education and funds research and development that enhances the safety of life at sea, on land and in the air.

REFERENCES

1. S. Wallbridge, A. Banford and A. Azapagic, Int J Life Cycle Assess, **18,** 2013, p 990-1008
2. R. Demmer, C. Boxall, *Radioactive Contamination Tenacity on Building Substrates*, Waste Management 2017, Conference Proceedings, WM Symposia, Temple, Arizona, 2017, Paper No. 17417, 14 pages, ISBN Number: 978-0-9828171-6-X
3. R.S. Hunter, *The Examination of Brickwork Removed From the Structural Containment of Plutonium Preparation Cells*, AEA Decommissioning & Radwaste, 1991, Ref No. PRC/RWM(91)49
4. J.B. Campbell, *Decommissioning of the B203 Plant at BNFL Sellafield*, BNFL, 1998, available at http://www.wmsym.org/archives/1998/html/sess31/31-03/31-03.htm
5. L. Bosworth-Waite and J. Rawcliffe, *Concrete and Brick Decontamination Options Assessment*, BNFL (NNL) internal report, 2005
6. P.R. Lutwyche and S.F. Challinor, *Sellafield Decommissioning Programme – Update and Lessons Learned*, British Nuclear Fuels Plc, 2003, presented at WM,03 Conference, February 23-27, 2003, Tucson, AZ
7. C. Phillips and A. Milliken, *Reprocessing as a Waste Management and Fuel Recycling Option*, Thorp Group, British Nuclear Fuels Plc, 2000, presented at WM'00 Conference, February 27 – March 2, 2000, Tucson, AZ
8. G.R. Howells, I.G. Hughes, D.R. Mackey, K. Saddington, *The Chemical Processing of Irradiated Fuels From Thermal Reactors*, 1958, Presented at, Second United Nations International Conference on the Peaceful Uses of Atomic Energy
9. L.W. Gray, K.S. Holliday, A. Murray, M. Thompson, D.T. Thorp, S. Yarbro, T.J. Venetz, *Separation of Plutonium from Irradiated Fuels and Targets*, Lawrence Livermore National Laboratory, 2015, Report for U.S. D.O.E.
10. C.M. Nicholls, *The Development of the Butex Process for the Industrial Separation of Plutonium from Nuclear Reactor Fuels*, J. British. Nuc. Energy, Vol **3**, No. 4, 1958, p279-289.
11. T. Todd, *Spent Nuclear Fuel Reprocessing*, Idaho National Laboratory, 2008, Presentation for, Nuclear Regulatory Commission Seminar Rockville, MD March 25, 2008, p 14.
12. Nuclear Energy Encyclopaedia: Science, Technology, and Applications, First Edition (Wiley Series On Energy), Edited by Steven B. Krivit, J.H. Lehr, and T.B. Kingery, 2011, John Wiley & Sons, Inc. Chapter 14.
13. M. Haleem Khan, A. Ali, Extraction of Thorium from Aqueous Nitric Acid Solutions by "Bis-2-(Butoxyethyl Ether) *(DBC)*, J. Rad. Nuc. Chem, Vol **203**, No. 1 ,1996, p 161-167
14. Materials Science and Engineering An Introduction, Seventh Edition, W.D. Callister, Jr, Edited by J. Hayton, 2010, John Wiley & Sons, Inc. p 480-81
15. O.M. Castellanos, C.A. Rios. , M.A. Ramos, E.V. Plaza, *A Comparative Study of Mineralogical Transformations in Fired Clays from the Laboyos Valley, Upper Magdalena Basin (Columbia)*, Boletín de Geología, Vol. **34**, No. 1, 2012, p 43-55
16. *Brick Clay, Mineral Planning Factsheet, British Geological Survey, 2007*
17. *Basic Civil Engineering, B.C. Punmia, 2004, Laxmi Publications p. 33, ISBN 978-81-7008-403-7*
18. A. De Bonis, G. Cultrone, C. Grifa, A. Langella, A.P. Leone, M. Mercurio, V. Morra, *Different shades of red: The complexity of mineralogical and physico-chemical factors influencing the colour of ceramics,* Ceramics International, **43**, 2017, p 8065–80747
19. G.S. Frankel, J.D. Vienna, J. Lian, J.R. Scully, S. Gin, J.V. Ryan, J. Wang, S.H. Kim, W. Windl and J. Du, *A Comparative Review of the Aqueous Corrosion of Glasses, Ceramics, and Metals*, Materials Degradation, Vol**. 2:15**, 2018; doi:10.1038/s41529-018-0037-2
20. C.M. Jantzen, K.G. Brown, and J.B. Pickett, *Durable Glass for Thousands of Years*, International Journal of Applied Glass Science, **1** [1], 2010, p 38–62 DOI:10.1111/j.2041-1294.2010.00007.x
21. Brick Industry Association, *Manufacturing of Brick*, Technical Notes on Brick Construction, **9**, 2006, p 5.
22. P.P. Poluektov, O.V. Schmidt, V.A. Kascheev and M.I. Ojovan, *Modelling aqueous corrosion of nuclear waste phosphate glass*, J. Nucl. Mater, **484**, 2017, p 357-366